Rare Metal Materials and Engineering
Volume 52, Issue 11, November 2023
Available online at www.rmme.ac.cn

Science Press

Cite this article as: Liu Guoqin, Lian Lixian, Liu Ying. Carbothermal Reduction Nitridation Reaction Assisted by Sol-Gel Method for CeN Powder Preparation[J]. Rare Metal Materials and Engineering, 2023, 52(11): 3730-3735. DOI: 10.12442/j.issn.1002-185X.20230238.

ARTICLE

Carbothermal Reduction Nitridation Reaction Assisted by Sol-Gel Method for CeN Powder Preparation

Liu Guoqin, Lian Lixian, Liu Ying

College of Materials Science and Engineering, Sichuan University, Chengdu 610065, China

Abstract: CeN powder was prepared through the carbothermal reduction nitridation reaction assisted by sol-gel method. Citric acid (CA) was used as the chelating agent, indicating that the organic material is used as the carbon source. The whole process could be divided into an aqueous phase process and a heat treatment process. The aqueous phase process mainly involved the chelation and polyester of Ce^{3+} and CA to form stable Ce^{3+}-CA chelate precursors. Homogeneous mixing at the molecular level of Ce and C sources could be achieved by the aqueous phase process. The heat treatment process included the in-situ carbonization and carbothermal reduction nitridation reaction. The in-situ carbonization process formed CeO_2/C powder, promoting the close contact between CeO_2 and C. The diffusion distance between the atoms of Ce and C sources is reduced to facilitate the carbothermal reduction nitridation process.

Key words: sol-gel; in-situ carbonization; carbothermal reduction nitridation reaction; CeN powder

Cerium nitride (CeN), as a rare earth mononitride, is the only semi-metallic conductor material among the rare earth-element-based compounds. CeN has excellent electromagnetic properties and special electronic valence characteristics: its effective valence state is between +3 and +4[1–3]. CeN can easily react with the oxygen, resulting in difficulties to prepare, store, and transport it, which greatly restricts its investigation and applications[4–5].

Conventionally, nitride powders are prepared by the carbothermal reduction nitridation reactions between solid reactants (metal oxides and solid carbon) and nitrogen source gas. Obviously, the homogeneous mixing of solid reactants is difficult, and the long-term reaction at high temperatures requires excellent heat resistance of the experimental equipment. It is reported that CeN can be obtained by the thin film preparation, which mainly uses radio-frequency ion plating and metal atom sputtering methods[6–9]. In these processes, the target poisoning easily occurs, which hinders or even terminates the sputtering process. Thus, CeN films can hardly form. Additionally, among the CeN powder preparation methods, the carbothermal reduction method takes precedence over nitridation synthesis[10–12] and novel reactive milling synthesis[13] methods. However, the obtained target products are multi-phase mixtures, and the content and purity of CeN should be further improved[14].

The sol-gel method is an effective low-temperature synthesis method with wide application in the synthesis of homogeneous metal oxides[15–18]. Different from the solid phase method, the sol-gel method is a typical wet chemical process, which can be used to prepare the homogeneous precursors with homogeneity at the atomic or molecular level[19–21]. The addition of chelating agent to the metal salt solution can form a stable and homogeneous metal chelate, and the target powder can be obtained after specific heat treatments[22–25].

In this research, the cerium nitrate hexahydrate $Ce(NO_3)_3\cdot 6H_2O$ and citric acid (CA) were used as the cerium source and organic carbon sources, respectively. The Ce^{3+}-CA precursors were prepared by sol-gel method, then treated by in-situ carbonization process to obtain CeO_2/C powder, and finally combined with carbothermal reduction nitridation reaction to prepare CeN powder.

1 Experiment

$Ce(NO_3)_3\cdot 6H_2O$ (AR) and CA (AR) were purchased from

Received date: April 24, 2023
Foundation item: National Double First-Class Universities Construction Grant of Sichuan University (2020SCUNG201)
Corresponding author: Lian Lixian, Ph. D., Professor, School of Materials Science and Engineering, Sichuan University, Chengdu 610065, P. R. China, E-mail: scu_lianyi@126.com

Sichuan Cologne Chemical Reagent Co., Ltd. Deionized water was used as the solvent in the experiments.

Firstly, $Ce(NO_3)_3 \cdot 6H_2O$ of fixed molar amount was added into the deionized water to obtain the solution with metal salt concentration of 1 mol/L. The solution was magnetically stirred to obtain a homogenous solution. Afterwards, CA was added to the obtained solution according to the molar ratio of $Ce(NO_3)_3 \cdot 6H_2O$ to CA as 1:1, 1:2, and 1:3. In this case, the molar ratio of $Ce(NO_3)_3 \cdot 6H_2O$ to CA is equal to the molar ratio of Ce^{3+} to CA. The mixed solution was magnetically stirred in water bath at 80 °C for 6 h to obtain uniform and stable Ce^{3+}-CA chelate. The Ce^{3+}-CA chelate was dried in a drying oven at 120 °C for 4 h. Due to the solvent evaporation and the decomposition of organic matter, a brownish webbed precursor material was obtained. The precursor was ground into powder, then placed in a small tube furnace, and treated at 600 °C for 2 h under the flowing high-purity Ar conditions to achieve the in-situ carbonization. Then, the obtained CeO_2/C powder was placed in a high-temperature tube furnace and treated at 1500 °C under high-purity N_2 atmosphere for 4 h, i.e., the CeO_2/C powder was treated through the carbothermal reduction nitridation reaction. Finally, the target product CeN powder was obtained after cooling to room temperature and it was stored in the glove box. The experiment process is shown in Fig.1.

The phase composition of the products was identified by X-ray diffractometer (XRD, DX-2700). All specimens were characterized by XRD with Mylar thin-film as a protective film. The morphology and component distribution of the products were investigated through the scanning electron microscope (SEM, JEOL JSM-7900F) equipped with energy dispersive spectroscope (EDS). The mechanism of organic precursor formation in the aqueous phase of sol-gels was investigated by Fourier transform infrared spectroscope (FTIR, INVENIO R). The in-situ carbonization process was analyzed by thermogravimetry (TG) and differential scanning calorimetry (DSC, PerkinElmer-STA8000). Raman spectra were obtained by laser Raman spectrometer (Raman, LabRAM HR).

2 Results and Discussion

2.1 Preparation of precursor powder by sol-gel method

In this research, the carbon source originates from CA, and the molar ratio of carbon greatly influences the phase composition of the product. The effect of molar ratio of Ce^{3+} to CA on the phase composition of the reaction products was investigated to optimize the experiment design and to improve the purity of CeN powder.

Fig. 2 shows XRD patterns of the Ce^{3+}-CA chelate precursors with different molar ratios of Ce^{3+} to CA. It can be seen that no significant diffraction peaks exist in the Ce^{3+}-CA chelate precursors, indicating that the chelate precursors are mainly amorphous structures. Fig.3 shows SEM morphologies of different precursor powders. When the molar ratio of Ce^{3+} to CA is 1: 1, some spongy porous structures appear. With increasing the CA concentration, the porous structure of the inner linkage gradually disappears and is transformed nto the block structure, as shown in Fig.3b–3c.

Fig.4 shows FTIR spectra of CA and Ce^{3+}-CA chelate precursors with different molar ratios of Ce^{3+} to CA. It can be seen from the CA spectrum that the peaks at 3492 and 3283 cm^{-1} are related to the -OH vibration and the vibration of O-H among water molecules, respectively. The peaks at 1743 and 1425 cm^{-1} correspond to the antisymmetric and symmetric vibrational peaks of C=O in the carboxyl group of CA, respectively. The peak at 1692 cm^{-1} corresponds to the stretching vibration peak of -COOH in CA. The characteristic peak of $-CH_2$ group appears in the range of 1430–1350 cm^{-1}. FTIR spectra of Ce^{3+}-CA chelate precursors are significantly different from that of pure CA. The vibrational absorption peak near 1610 cm^{-1} corresponds to the symmetric stretching vibrational peak of C=O bond in the ionized carboxyl group (-COO). The vibrational absorption peak of NO^{3-} and the symmetric peak of C=O can be observed in the range of 1390–1370 cm^{-1}. The peaks in the range of 1090 – 1030 cm^{-1} are

Fig.1 Experiment process of CeN preparation through carbothermal reduction nitridation reaction assisted by sol-gel method

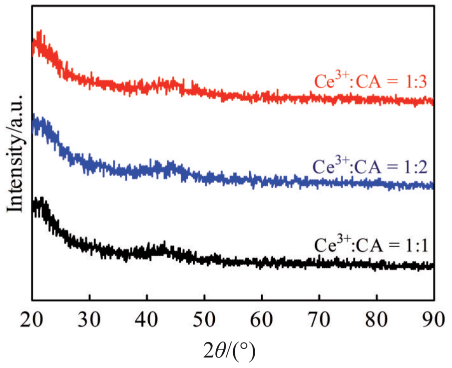

Fig.2 XRD patterns of Ce^{3+}-CA chelate precursors with different molar ratios of Ce^{3+} to CA

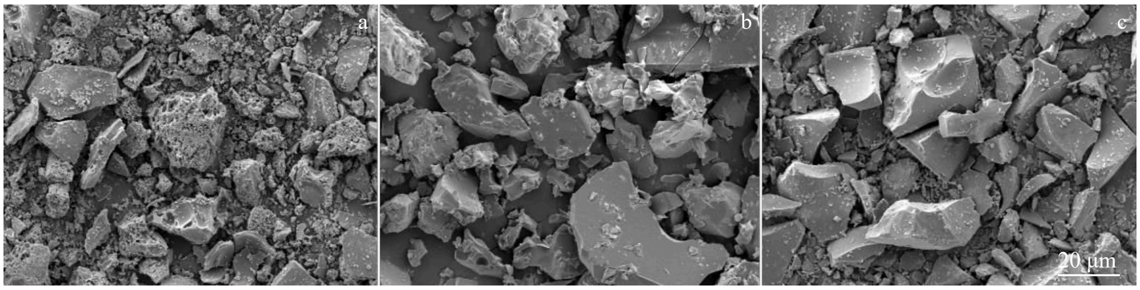

Fig.3 SEM morphologies of Ce^{3+}-CA chelate precursors with different molar ratios of Ce^{3+} to CA: (a) 1:1, (b) 1:2, and (c) 1:3

related to the vibrational absorption peaks of C-O-C-. The peak intensity of NO^{3-} and C-O-C- is gradually weakened with increasing the CA concentration in the preparation.

As shown in Fig. 4, the disappearance of -OH, O-H, and carboxyl C=O stretching vibration peaks of CA, the weakening of the antisymmetric stretching peak of C=O, and the appearance of NO^{3-} and C-O-C- vibration absorption peaks all indicate the occurrence of polyester reaction, i. e., Ce^{3+} interacts with the hydroxyl and carboxyl groups of CA, forming the Ce^{3+}-CA chelate. The formation of the chelate structure promotes the immobilization of Ce^{3+} in the three-dimensional network structure of the organic precursor. Thus, the homogeneous mixing at molecular scale is achieved and the required diffusion distance between the atoms of Ce and C sources is reduced. Briefly, the in-situ carbonization process forms CeO_2/C powder with increasing the contact area of CeO_2 and C, therefore reducing the migration distance between Ce and C atoms in the carbothermal reduction nitridation reaction, which promotes the CeN preparation at 1500 °C during carbothermal reduction nitridation process.

2.2 In-situ carbonization of precursor powder

TG-DSC curves of the representative precursor powder are displayed in Fig.5. With increasing the temperature from room temperature to 600 °C, a series of exothermic peaks appear in DSC curve (curve of heat flow) and significant mass loss can be observed in TG curve (curve of remained mass).

As shown in Fig. 5, there are four stages of mass loss with increasing the temperature. The first stage is that partial crystallization water molecules leave the $Ce(NO_3)_3·6H_2O$ compound at temperatures from room temperature to 70 °C, therefore forming $Ce(NO_3)_3·4H_2O$. The second stage occurs at 70–142 °C, where the adsorbed and crystallized water of the material continues to evaporate, thereby forming $Ce(NO_3)_3·H_2O$. The third stage is at 142–353 °C, where the last crystallization water is removed, thus forming $Ce(NO_3)_3$. Subsequently, the in-situ carbonization gradually occurs to form CeO_2. Meanwhile, the thermal decomposition of CA and the oxidative decomposition of CA-related composites occur. The fourth stage occurs at 353 – 634 ° C, which mainly consists of the decomposition of nitrate and organic matter as well as the in-situ carbonization of precursors. It is clear that the thermal treatment of sol-gel precursors consists of two main parts: one is the water evaporation, including the adsorbed and crystallized water; the other is the decomposition of organic matter and in-situ carbonization of precursor.

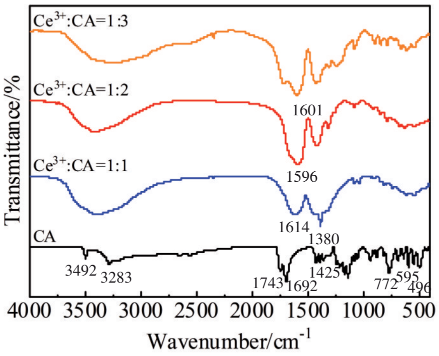

Fig.4 FTIR spectra of CA and Ce^{3+}-CA chelate precursors with different molar ratios of Ce^{3+} to CA

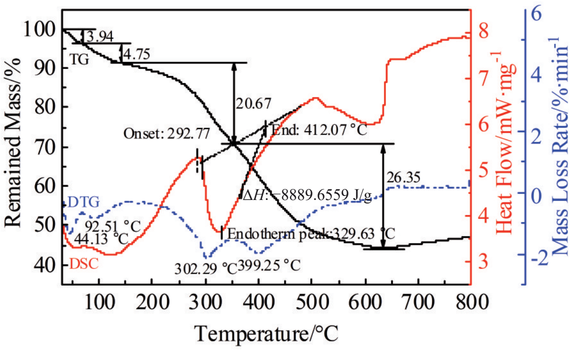

Fig.5 TG-DSC curves of representative precursor powder

Fig. 6 shows XRD patterns of the in-situ carbonization products of precursor with different molar ratios of Ce^{3+} to CA. A distinctive diffraction peak of CeO_2 can be observed in the in-situ carbonization product with molar ratio of Ce^{3+}:CA=1:1. When the molar ratio of Ce^{3+} to CA is 1:2 and 1:3, some weaker and wider diffraction peaks can be observed, and they may be related to the CeO_2 diffraction peaks. This phenomenon indicates the formation of CeO_2 with poor crystalline phase when the molar ratio of Ce^{3+} to CA is 1:2 and 1:3. In other words, CeO_2 exists in the in-situ carbonization products. No diffraction peaks of carbon can be observed in Fig.6, inferring that the carbon exists in the amorphous form at this stage. With increasing the molar ratio of Ce^{3+} to CA, the

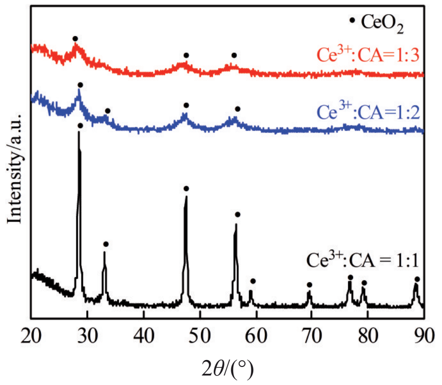

Fig.6 XRD patterns of in-situ carbonization products of precursors with different molar ratios of Ce^{3+} to CA

intensity of the diffraction peaks is gradually reduced. This is probably because with increasing the CA concentration, the thickness of the amorphous carbon layer on the product surface is gradually increased, which leads to the decrease in the intensity of CeO$_2$ diffraction peaks. SEM morphologies of the in-situ carbonization products of precursor with different molar ratios are shown in Fig.7, which basically maintain the characteristics of the precursor powders (Fig. 3). The more clear porous structure of the products in Fig.7a may be caused by the continuous release of gas during the in-situ carbonization.

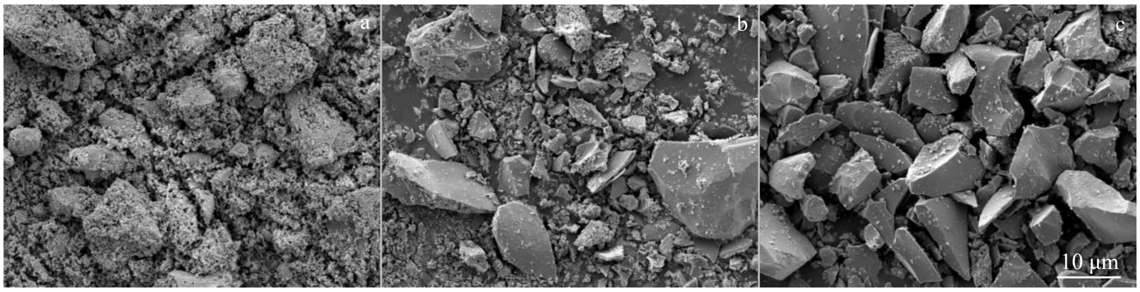

Fig.7 SEM morphologies of in-situ carbonization products of precursors with different molar ratios of Ce^{3+} to CA: (a) 1:1, (b) 1:2, and (c) 1:3

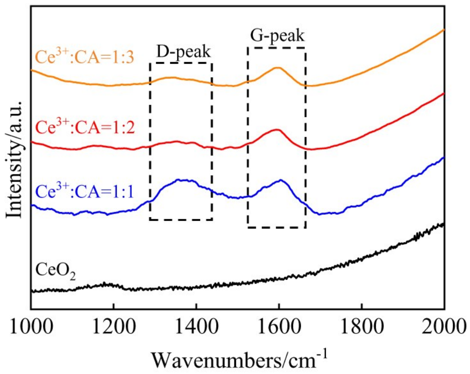

Fig.8 Raman spectra of pure CeO$_2$ and in-situ carbonization products with different molar ratios of Ce^{3+} to CA

Fig. 8 shows the Raman spectra of pure CeO$_2$ powder and in-situ carbonization products with different molar ratios of Ce^{3+} to CA. No peak of carbon can be observed in the Raman spectrum of pure CeO$_2$. However, two distinctive Raman peaks of disordered amorphous carbon, D-peak and G-peak, exist in the in-situ carbonization products with different molar ratios of Ce^{3+} to CA. The D-peak near 1350 cm^{-1} indicates the boundary vibration mode of the hexagonal Brillouin zone induced by disorder, which is mainly caused by the material defects. The larger the D-peak intensity, the more the defects in the material[26]. It can be seen that the D-peak intensity is gradually decreased with changing the molar ratio of Ce^{3+} to CA from 1: 1 to 1: 3. Therefore, it can be inferred that the defects in the in-situ carbonization products are gradually reduced with increasing the CA concentration. The G-peak near 1580 cm^{-1} suggests the stretching vibration mode of the bonds within the carbon atom (sp^2) plane, which is related to the graphitization degree. The presence of D-peak and G-peak indicates the existence of carbon in the in-situ carbonization specimens and the formation of a strong bond between CeO$_2$ and carbon.

To further demonstrate the existence of carbon in the in-situ carbonization products and to investigate the distribution of the product elements, EDS analysis was conducted based on the in-situ carbonization product with molar ratio of Ce^{3+}:CA= 1: 3 and the results are shown in Fig. 9. The in-situ carbonization specimen only contains Ce, O, and C elements. It can be seen that Ce, O, and C elements are uniformly distributed in the specimen. Therefore, it can be inferred that the in-situ carbonization product CeO$_2$ is uniformly distributed in the cleaved C matrix. The distributions of Ce, O, and C elements in the in-situ carbonization products with molar ratio of Ce^{3+} to CA as 1:1 and 1:2 are similar to those in Fig.9.

2.3 Carbothermal reduction nitridation reaction

XRD patterns of the products after carbothermal reduction nitridation reaction are shown in Fig.10. When the molar ratio of Ce^{3+} to CA is 1: 1, the carbothermal reduction nitridation reaction product is a mixture of Ce$_2$O$_3$, Ce$_2$ON$_2$, and CeN. When the molar ratio of Ce^{3+} to CA is 1: 2, the diffraction peaks of Ce$_2$O$_3$ and Ce$_2$ON$_2$ phases disappear and only the diffraction peaks of CeN phase exist. The C content further increases when the molar ratio of Ce^{3+} to CA is 1:3, and the product is still the CeN phase. As shown in Fig. 10, with increasing the C content, the CeN peak intensity is decreased,

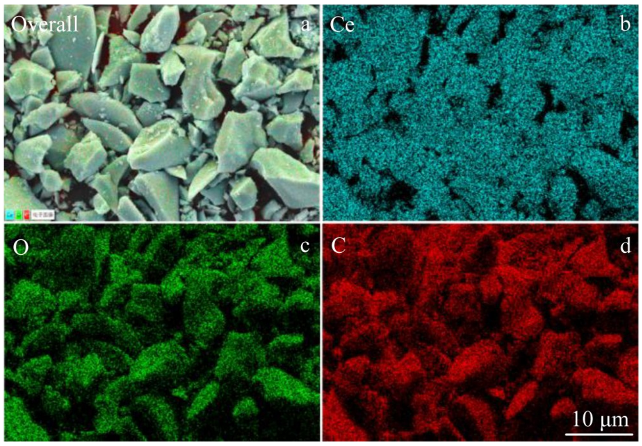

Fig.9 SEM morphology (a) and EDS mapping results of Ce (b), O (c), C (d) elements of in-situ carbonization product with molar ratio of Ce^{3+}:CA=1:3

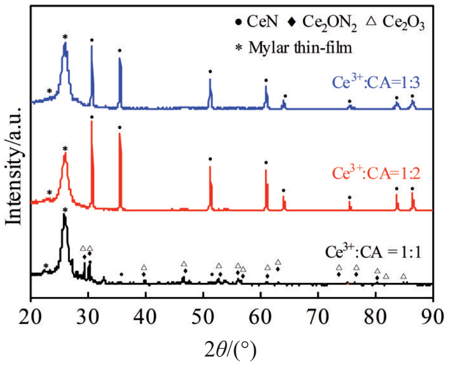

Fig.10 XRD patterns of carbothermal reduction nitridation reaction products with different molar ratios of Ce^{3+} to CA

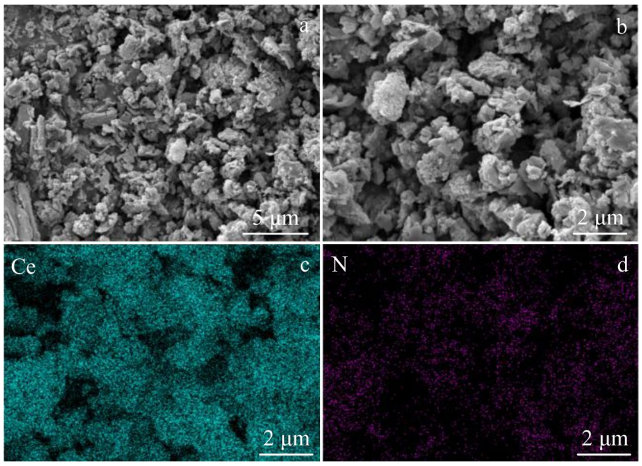

Fig.11 SEM morphologies of carbothermal reduction nitridation reaction products with molar ratio of Ce^{3+} to CA as 1:2 (a–b); EDS mapping results of Ce (c) and N (d) elements corresponding to Fig.11b

indicating that the crystallinity of CeN decreases. Additionally, the excess increase in initial CA content leads to the excess carbon in the carbothermal reduction nitridation products. Therefore, the molar ratio of Ce^{3+} to CA of 1:2 is the optimal parameter for the preparation of CeN powder through the carbothermal reduction nitridation reaction assisted by sol-gel method.

SEM morphologies and EDS element mappings of the carbothermal reduction nitridation reaction products with molar ratio of Ce^{3+} to CA as 1:2 are shown in Fig. 11. As shown in Fig.11a–11b, the micron-sized powder with irregular and massive morphology can be observed. In addition, the agglomerative sintering between the powder particles occurs. Mainly Ce and N elements can be detected, as shown in Fig. 11c – 11d. It is found that both Ce and N elements are homogeneously distributed.

3 Conclusions

1) CeN powder can be prepared by the carbothermal reduction nitridation reaction assisted by sol-gel method, using $Ce(NO_3)_3 \cdot 6H_2O$ as the cerium source and citric acid (CA) as the chelating agent. This method uses organic carbon as the carbon source instead of conventional solid carbon.

2) The preparation process can be divided into two main stages. One is the aqueous phase Ce^{3+}-CA chelation stage, which achieves the homogeneous mixing of the Ce source with C source at the molecular level. The other is the heat treatment stage, which includes the in-situ carbonization to obtain CeO_2/C powder and carbothermal reduction nitridation reaction to obtain CeN powder.

3) The in-situ carbonization process forms CeO_2/C powder through increasing the contact area of CeO_2 and C, therefore reducing the migration distance between Ce and C atoms in the carbothermal reduction nitridation reaction, which promotes the CeN preparation at 1500 °C during carbothermal reduction nitridation process.

References

1 Olcese G L. *Journal of Physics F: Metal Physics*[J], 1979, 9(3): 569

2 Patthey F, Cattarinussi S, Schneider W D *et al. Europhysics Letters*[J], 1986, 2(11): 883

3 Aerts C M, Strange P, Horne M *et al. Physical Review B*[J], 2004, 69(4): 5115

4 Norman M R, Koelling D D, Freeman A J *et al. Physical Review Letters*[J], 1984, 53(17): 1673

5 Norman M R, Wimmer E, Freeman A J. *Physical Review B*[J], 1985, 32(12): 7830

6 Yue W, Taimin Y, Fu Y J *et al. Surface & Coatings Technology*[J], 2020, 381: 125 168

7 Xiao S Q, Takai O. *Thin Solid Films*[J], 1998, 317(1–2): 137

8 Xiao S Q, Tsuzuki K, Lungu C P *et al. Vacuum*[J], 1998, 51(4): 691

9 Xiao W, Guo Q, Wang E G. *Journal of Physical Chemistry B*[J], 2005, 109(11): 4953

10 Nakagawa T, Matsuoka H, Sawa M *et al. Journal of Nuclear*

Materials[J], 1997, 247: 127

11 Nakagawa T, Matsuoka H, Sawa M *et al. Journal of Nuclear Materials*[J], 1997, 247: 147

12 Hirota M, Katsura M, Miyake M. *Journal of Alloys and Compounds*[J], 1994, 207–208: 409

13 Callahan P G, Jaques B J, Marx B M. *Journal of Nuclear Materials*[J], 2009, 392(1): 121

14 Butt D P, Jaques B. *Synthesis and Optimization of the Sintering Kinetics of Actinide Nitrides*[R]. Boise: Boise State University, 2009

15 Fernandes J D G, Melo D M A, Zinner L B *et al. Materials Letters*[J], 2002, 53(1–2): 122

16 Kwon H T, Bukhovko M P, Mahamulkar S *et al. AIChE Journal*[J], 2018, 64(11): 4019

17 Ma J X, Hong Y Z, Sun Y Z *et al. Nuclear Analysis*[J], 2022, 1(1): 100 008

18 Alanazi H M, AlHaddad M, Shawky A *et al. Catalysis Communications*[J], 2023, 177: 106 646

19 Cushing B L, Kolesnichenko V L, O'Connor C J. *Chemical Reviews*[J], 2004, 104(9): 3893

20 Danks A E, Hall S R, Schnepp Z. *Materials Horizons*[J], 2016, 3(2): 91

21 Zhao Shijiao, Ma Jingtao, Zhao Xingyu *et al. Rare Metal Materials and Engineering*[J], 2020, 49(2): 732 (in Chinese)

22 Yan C L, Liu R J, Zhang C R *et al. RSC Advances*[J], 2015, 5(46): 63 520

23 Guo H X, Wang J R, Bai J *et al. Journal of the American Ceramic Society*[J], 2018, 101(7): 2786

24 Wang Weichao, Liu Gu, Wang Liuying *et al. Rare Metal Materials and Engineering*[J], 2022, 51(3): 1003 (in Chinese)

25 Ouyang L F, Yang X J, Li X L *et al. Rare Metal Materials and Engineering*[J], 2022, 51(6): 2039

26 Ferrari A C, Meyer J C, Scardaci V *et al. Physical Review Letters*[J], 2006, 97(18): 187 401

溶胶-凝胶法辅助碳热还原氮化反应制备CeN粉末

刘国琴，连利仙，刘　颖

(四川大学 材料科学与工程学院，四川 成都 610065)

摘　要：以柠檬酸（CA）为螯合剂，即以有机物为碳源，通过溶胶-凝胶法辅助碳热还原氮化反应制备了CeN粉末。整个反应过程分为水相过程和热处理过程。水相过程主要是Ce^{3+}和CA的螯合和聚酯，形成稳定的Ce^{3+}-CA螯合物前驱体。通过水相过程实现Ce源与C源在分子水平上的均匀混合。热处理过程包括原位碳化和碳热还原氮化反应两部分。原位碳化过程形成的CeO_2/C粉末促进了CeO_2和C之间的紧密接触，从而减少Ce源和C源原子的扩散距离，以促进碳热还原氮化过程。

关键词：溶胶-凝胶；原位碳化；碳热还原氮化反应；CeN粉末

作者简介：刘国琴，女，1997年生，硕士，四川大学材料科学与工程学院，四川 成都 610065，电话：028-85405332，E-mail：jean1150791451@163.com